



Published in final edited form as:

*J Magn Reson.* 2007 February ; 184(2): 350–356.

## Sensitivity Enhancement in $^{13}\text{C}$ Solid-State NMR of Protein Microcrystals by Use of Paramagnetic Metal Ions for Optimizing $^1\text{H}$ $T_1$ Relaxation

Nalinda P. Wickramasinghe<sup>a</sup>, Mrignayani Kotecha<sup>a</sup>, Ago Samoson<sup>b</sup>, Jaan Past<sup>b</sup>, and Yoshitaka Ishii<sup>a,\*</sup>

<sup>a</sup> Department of Chemistry, University of Illinois at Chicago 845 W Taylor St., Chicago IL 60607, USA

<sup>b</sup> National Institute of Chemical Physics and Biophysics, Akadeemia tee 23, 12618 Tallinn, Estonia

### Abstract

We discuss a simple approach to enhance sensitivity for  $^{13}\text{C}$  high-resolution solid-state NMR for proteins in microcrystals by reducing  $^1\text{H}$   $T_1$  relaxation times with paramagnetic relaxation reagents. It was shown that  $^1\text{H}$   $T_1$  values can be reduced from 0.4–0.8 s to 60–70 ms for ubiquitin and lysozyme in  $\text{D}_2\text{O}$  in the presence of 10 mM  $\text{Cu(II)Na}_2\text{EDTA}$  without substantial degradation of the resolution in  $^{13}\text{C}$  CPMAS spectra. Faster signal accumulation using the shorter  $^1\text{H}$   $T_1$  attained by paramagnetic doping provided sensitivity enhancements of 1.4–2.9 for these proteins, reducing the experimental time for a given signal-to-noise ratio by a factor of 2.0–8.4. This approach presented here is likely to be applicable to various other proteins in order to enhance sensitivity in  $^{13}\text{C}$  high-resolution solid-state NMR spectroscopy.

### Keywords

solid-state NMR; protein microcrystal;  $T_1$  relaxation; paramagnetic doping;  $^{13}\text{C}$  CPMAS

### Introduction

Over the past years, significant progress has been achieved in solid-state NMR (SSNMR) spectroscopy of biomolecules such as peptides and proteins.[1–16] Particularly, use of protein micro-/nano-crystals[17] has significantly improved resolution in high-resolution SSNMR of dilute spins such as  $^{13}\text{C}$  and  $^{15}\text{N}$ , permitting signal assignment and structural determination of various uniformly  $^{13}\text{C}$  and/or  $^{15}\text{N}$ -labeled proteins by SSNMR.[18–25] However, restricted sensitivity in  $^{13}\text{C}$  and  $^{15}\text{N}$  SSNMR has been still one of the major limiting factors in SSNMR analysis of proteins. In an experimental time required for  $^{13}\text{C}$  SSNMR of proteins, more than 95 % is typically consumed for recycle delays to retrieve spin polarization by  $^1\text{H}$   $T_1$  relaxation, to protect a probe from arcing due to RF irradiation, or to avoid sample degradation due to heating. The latter two problems have been addressed by improving designs of MAS probes to minimize sample heating[26] and tolerate handling of relatively high RF power,[27] or by using low-power  $^1\text{H}$  decoupling.[28;29] Doping with paramagnetic metal ions such as  $\text{Cu(II)}$  has been utilized to reduce  $^1\text{H}$   $T_1$  relaxation times in  $^{13}\text{C}$  CPMAS of proteins/peptides in

\*To whom the correspondence should be addressed. E-mail: yishii@uic.edu Phone: 312-413-0076 Fax: 312-996-0431

**Publisher's Disclaimer:** This is a PDF file of an unedited manuscript that has been accepted for publication. As a service to our customers we are providing this early version of the manuscript. The manuscript will undergo copyediting, typesetting, and review of the resulting proof before it is published in its final citable form. Please note that during the production process errors may be discovered which could affect the content, and all legal disclaimers that apply to the journal pertain.

cryogenic conditions.[30] However, the effects of paramagnetic doping on resolution and  $T_1$  relaxation have not been fully examined for biomolecular SSNMR, in particular, for  $^{13}\text{C}$  CPMAS of protein micro-crystals, which generally provides excellent resolution.

In this study, we experimentally investigate the effects of paramagnetic ion doping to reduce  $^1\text{H}$   $T_1$  values in 1D  $^{13}\text{C}$  CPMAS for microcrystals of two model proteins: ubiquitin and lysozyme using a  $\text{Cu(II)Na}_2\text{EDTA}$  complex (Cu-EDTA) as a relaxation reagent. In addition to  $^1\text{H}$   $T_1$  values, we examine resolution and line positions in  $^{13}\text{C}$  CPMAS spectra for these proteins in the presence of Cu-EDTA. Motivations and prospects of this approach for sensitivity enhancements in biomolecular SSNMR are presented.

## Materials and Methods

$\text{D}_2\text{O}$  was purchased from Cambridge isotope (Andover, MA). Ubiquitin from bovin red blood cells (ubiquitin), lysozyme from chicken egg white (lysozyme), and other chemicals were purchased from Sigma-Aldrich (St. Louis, MO). Purified water (double deionized and distilled) was prepared using a High-Q 103 S water still system (High-Q Corp., Wilmette, IL). The purified water was used for preparation of all the protein microcrystals in  $\text{H}_2\text{O}$ .

We prepared protein microcrystals in  $\text{D}_2\text{O}$  or  $\text{H}_2\text{O}$  following the protocols by Martin and Zilm for preparing protein nanocrystals[17] with minor modifications. Unless otherwise mentioned, all the data were collected for samples prepared in  $\text{D}_2\text{O}$  for potential applications to partially deuterated proteins in  $\text{D}_2\text{O}$ . As will be discussed, protein microcrystals prepared in  $\text{D}_2\text{O}$  have longer  $^1\text{H}$   $T_1$  values than those in  $\text{H}_2\text{O}$ . Thus, the effects of paramagnetic doping are more notable for proteins in  $\text{D}_2\text{O}$ , although this approach is also effective for samples prepared in  $\text{H}_2\text{O}$ . An equal volume mixture of a protein stock solution (25 mg protein/ml) and a crystallization solution was concentrated to approximately half the starting volume by using a SpeedVac concentrator (Savant, Farmingdale, NY).[17] For preparation of the protein stock solution, lysozyme was dissolved in a 100 mM sodium acetate buffer (pH 4.5) while ubiquitin was dissolved in pure  $\text{D}_2\text{O}/\text{H}_2\text{O}$ . The crystallization solution for ubiquitin contained 25% w/v PEG 8000 and 200 mM cadmium acetate in a 50 mM sodium HEPES buffer (pH 7); the solution for lysozyme contained 12.5% w/v PEG 2000 and 75 mM sodium chloride in a 100 mM sodium acetate buffer (pH 4.5). The concentrated protein solution of ~0.5 mL was kept in a microtube at 4 °C for 10-12 hours to produce protein crystals. Then, the solution containing crystals was centrifuged at  $1.5 \times 10^3$  g for 5 min using an Eppendorf 5414D micro-centrifuge (Eppendorf, Westbury, NY).

A Cu-EDTA complex was selected as a relaxation reagent that minimizes undesired interactions between metal ions and proteins.[31] To prepare protein crystal samples containing Cu-EDTA, about 0.4 mL of the mother liquor was separated as a supernatant from the protein crystals after the centrifugation. Then, 1.0-14.9 mg of Cu-EDTA was dissolved in the mother liquor. This solution was kept at 4 °C for 2-4 hours, and centrifuged to remove any precipitated proteins due to the salts. After the pH was adjusted to an appropriate value for the particular protein, the mother liquor containing Cu-EDTA was reintroduced to the protein crystals, and left at 4 °C for another 10-12 hours to dope Cu-EDTA into protein crystals. The samples which do not contain Cu-EDTA were prepared in the same manner for a control, but without the addition of Cu-EDTA. Then, the sample was centrifuged for 5 min, and the collected protein crystals were packed into a MAS rotor by centrifugation. The concentration of Cu-EDTA was estimated from the amount of Cu-EDTA used and the total volume of the mother liquor and the protein microcrystals. Formation of the protein crystals were confirmed under an optical microscope. The images of the crystals were obtained at  $\times 32$  magnification using a CCD camera (CoolSnap, Roper, Trenton, NJ) attached to a Carl Zeiss Axiovert 25 inverted microscope (Carl Zeiss MicroImaging, Thornwood, NY).

SSNMR experiments were performed at 9.4 T ( $^1\text{H}$  NMR frequency of 400.2 MHz) with a Varian InfinityPlus 400 NMR spectrometer. For experiments at the spinning of 10 kHz, a Varian T3 3.2-mm MAS double-resonance NMR probe or a home-built 2.5-mm MAS double-resonance probe was used. The signals were collected during an acquisition period of 10 ms at the spinning speed of  $10,000 \pm 5$  Hz with cooling air at  $-10$  °C supplied through a Varian VT stack at a flow rate of  $\sim 140$  standard-cubic-feet per hour (scfh). For experiments at the spinning of 40 kHz, we used a 2.0-mm MAS double-resonance probe developed in Dr. Samoson's lab.[32-34] Unless otherwise mentioned, the signals were collected during an acquisition period of 20 ms at the spinning speed of  $40,000 \pm 10$  Hz with cooling air at  $-5$  °C supplied through the Varian VT stack at a flow rate of  $\sim 140$  scfh and cooled bearing air ( $1$  °C). The data were processed with Varian Spinsight software. The spectra in Fig 2 were processed with Gaussian line broadening of 15 Hz; other spectra were processed with Gaussian line broadening of 25 Hz.  $^1\text{H}$   $T_1$  values were calculated from the data collected by  $^1\text{H}$  inversion recovery experiments detected by  $^{13}\text{C}$  CPMAS, where a  $\pi$ -pulse to  $^1\text{H}$  spins and the following inversion recovery delay were added prior to the conventional CPMAS sequence with ramped CP[35] and TPPM decoupling[36]. The signal intensities were measured for the highest signals in the  $^{13}\text{CO}$  (160-190 ppm),  $^{13}\text{Ca}$  (40-65 ppm),  $^{13}\text{CH}$  (10-30 ppm) regions to estimate  $^1\text{H}$   $T_1$ ; the average of the  $^1\text{H}$   $T_1$  values estimated for the three regions was used as  $^1\text{H}$   $T_1$  of the sample. For proteins without Cu-EDTA, some variations in  $^1\text{H}$   $T_1$  values ( $\sim 10$  %) were observed from batch to batch. We also noticed that  $^1\text{H}$   $T_1$  is gradually reduced (10-25 %) over the course of experiments after a week for the proteins without Cu-EDTA. The values for  $^1\text{H}$   $T_1$  in Table 1 were measured within a week after the sample was packed in a rotor.

## Results and Discussion

In Fig. 1(a-d), we demonstrate sensitivity enhancements in  $^{13}\text{C}$  CPMAS by faster signal accumulation using short  $^1\text{H}$   $T_1$  optimized with Cu-EDTA doping for (a, b) lysozyme and (c, d) ubiquitin microcrystals. These spectra were collected (a, c) with 10 mM Cu-EDTA and (b, d) without Cu-EDTA in a common experimental time of 4 hours. Inspections of the microscopic images in Fig. 1(e-h) for the crystals (e, g) with and (f, h) without Cu-EDTA revealed that there were no noticeable changes in the crystal shapes or sizes due to the introduction of Cu-EDTA for (e, f) lysozyme and (g, h) ubiquitin. Hence, it is not likely that the addition of Cu-EDTA damaged the protein crystals. The recycle delays for the lysozyme samples were (a) 0.5 s ( $^1\text{H}$   $T_1 = 59$  ms) and (b) 1.1 s ( $^1\text{H}$   $T_1 = 350$  ms) while the delays for the ubiquitin samples were (c) 1.0 s ( $^1\text{H}$   $T_1 = 73$  ms) and (d) 2.5 s ( $^1\text{H}$   $T_1 = 820$  ms). As will be discussed later, increasing the Cu-EDTA concentration further reduces  $^1\text{H}$   $T_1$  values. For comparison, the spectra were scaled so that the spectra for the same protein display a common noise level. Faster signal accumulation using the shorter  $^1\text{H}$   $T_1$  in the presence of Cu-EDTA clearly yielded considerable sensitivity enhancements by factors of 1.4 and 1.6 in Fig. 1(a) and (c), respectively. It is also clear that no major changes in the line positions or line-widths were induced by the presence of 10 mM Cu-EDTA. Since line positions in  $^{13}\text{C}$  CPMAS spectra were not altered by the Cu-EDTA doping, major structural changes in the proteins due to Cu-EDTA doping are not likely.  $^1\text{H}$   $T_1$  values were successfully reduced by a factor of 6-11. On the other hand, we were able to speed up the experiment by only up to 2.5 times to protect a probe from arcing under high-power  $^1\text{H}$  RF decoupling. We also tested decoupling by fast MAS at 20-30 kHz, which was successfully employed in our recent studies for paramagnetic systems.[37-39] However, the resolution without  $^1\text{H}$  RF decoupling is considerably limited for the diamagnetic polycrystalline proteins.

To overcome this problem, we employed a rotor-synchronous  $\pi$ -pulse train decoupling under ultra-fast MAS condition (40 kHz), which was recently proposed by Hafner and coworkers at Varian.[40] We found that this decoupling permits narrowing comparable to TPPM decoupling of  $^1\text{H}$  RF irradiation at 200 kHz under MAS at 40 kHz. An equivalent decoupling sequence

was successfully applied for  $^1\text{H}$  decoupling for paramagnetic systems[39] and  $^{19}\text{F}$  decoupling for fluoro-polymers[41] under fast MAS ( $\geq 20$  kHz). Figure 2 shows CPMAS spectra at a spinning speed of 40 kHz for (a, b) lysozyme and (c, d) ubiquitin microcrystals (a, c) with and (b, d) without 10 mM Cu-EDTA doping. The recycle delays for the lysozyme samples were (a) 0.18 s ( $^1\text{H } T_1 = 60$  ms) and (b) 1.5 s ( $^1\text{H } T_1 = 500$  ms) while the delays for the ubiquitin samples were (c) 180 ms ( $^1\text{H } T_1 = 60$  ms) and (d) 2.5 s ( $^1\text{H } T_1 = 820$  ms). We confirmed that faster signal accumulation with the low-duty-factor  $^1\text{H}$  decoupling sequence at a spinning speed of 40 kHz further enhanced sensitivity in the  $^{13}\text{C}$  CPMAS spectra by a factor of 2.7-2.9, which speeds up our experiments 7-8 fold. The resolution of the CPMAS spectra obtained with fast recycling in the presence of Cu-EDTA was comparable to that without Cu-EDTA. It is noteworthy that the effective RF duty factor due to  $^1\text{H}$  decoupling is only  $\sim 1.1\%$  in the experiment with a recycle delay of 180 ms and an acquisition period of 20 ms. Because of the low RF duty factor and high efficiency of the  $^1\text{H}$  RF circuit of the fast MAS probe, we could collect the signals up to 30 ms of acquisition periods without any arcing problems. Thus, significant sensitivity enhancements with uncompromised resolution in this approach are possible under the fast MAS condition.

We prepared crystals in  $\text{D}_2\text{O}$  and  $\text{H}_2\text{O}$  without Cu-EDTA to examine solvent effects on  $^1\text{H } T_1$  values. Considerably longer  $^1\text{H } T_1$  was observed in  $\text{D}_2\text{O}$  for ubiquitin and, to a lesser degree, for lysozyme, as shown in Table 1. The sensitivity enhancements for the proteins in  $\text{H}_2\text{O}$  are less, particularly for ubiquitin. Nevertheless, considerable sensitivity gains ( $\sim 2$ ) are still expected under the fast MAS and decoupling condition used for Fig. 2. Martin and Zilm reported that  $^1\text{H } T_1$  of unlabeled ubiquitin nanocrystals in  $\text{H}_2\text{O}$  is 0.5 s.[17] Zilm and coworkers more recently reported average  $^1\text{H } T_1$  values of 300-400 ms for uniformly  $^2\text{D}$ - and  $^{15}\text{N}$ -labeled ubiquitin nanocrystal samples for which amide protons are back-exchanged in  $\text{H}_2\text{O}$ , as well as for unlabeled ubiquitin.[42] Thus, the long  $^1\text{H } T_1$  observed for our ubiquitin sample in  $\text{D}_2\text{O}$  cannot be simply explained by lower  $^1\text{H}$  density. Understanding this solvent dependence of  $^1\text{H } T_1$  requires more systematic work, and a fuller study is outside of the scope of this study.

Figure 3 shows  $^{13}\text{C}$  CPMAS spectra of ubiquitin microcrystals acquired at different  $^1\text{H}$  inversion recovery delays (a) without and (b) with 10 mM Cu-EDTA. This result clearly shows that the  $^1\text{H } T_1$  value of lysozyme is reduced by the introduction of Cu-EDTA in a uniform manner for different chemical groups and residues. After 50 ms, the  $^{13}\text{C}$  CPMAS spectra in (b) display a null signal in the presence of Cu-EDTA, while the spectra in (a) show a signal close to the null only after 800 ms without Cu-EDTA.  $^1\text{H } T_1$  values obtained from the experiments are (a) 830 ms and (b) 73 ms. In a recent study on uniformly  $^{13}\text{C}$  labeled ubiquitin by Igumenova *et. al.*, it has been reported that a 2D  $^{13}\text{C}/^{13}\text{C}$  chemical-shift correlation experiment at  $^1\text{H}$  frequency of 800 MHz required about 36 hours with recycle delay of 1.5 s. [43] Assuming that the RF-duty factor and the sample stability are not the limiting factor, it is possible to speed up this experiment up to seven times with a shorter  $^1\text{H } T_1$  value of  $\sim 70$  ms in the paramagnetic doping approach.

Figure 4 shows Cu-EDTA concentration dependence of the longitudinal relaxation rate  $1/T_1$  for the lysozyme sample. Figure 4 clearly demonstrates that  $1/T_1$  is not linearly proportional to the concentration of Cu-EDTA. The slope is the largest at the lower Cu-EDTA concentration (5-10 mM). At higher concentration, the relaxation rate increases more slowly for a given increase in the Cu-EDTA concentration. This is probably because  $^1\text{H } T_1$  relaxation due to the paramagnetic reagents is mediated by a  $^1\text{H}$ - $^1\text{H}$  spin diffusion mechanism.[44] Since Cu-EDTA is hydrophilic, it is most likely that  $^1\text{H}$  polarization is retrieved more quickly by paramagnetic  $T_1$  relaxation around the water-accessible protein surface, where Cu-EDTA is easily accessible. The recovered polarization can be transferred across the molecule by  $^1\text{H}$ - $^1\text{H}$  spin diffusion. We noticed that there is minor solvent dependence of  $^1\text{H } T_1$  even in the presence of Cu-EDTA. Slightly lower  $^1\text{H } 1/T_1$  rates in  $\text{D}_2\text{O}$  may be attributed to slower  $^1\text{H}$ - $^1\text{H}$  spin diffusion in  $\text{D}_2\text{O}$ ,

in which amide hydrogens are exchanged for  $^2\text{D}$ . In spite of the difference, we found that in both  $\text{H}_2\text{O}$  and  $\text{D}_2\text{O}$  solvents,  $^1\text{H } T_1$  for the protein microcrystal samples can be reduced to 20-30 ms in the presence of 75 mM Cu-EDTA.

In Fig. 5, we examined resolution of  $^{13}\text{C}$  CPMAS spectra for (a, b) lysozyme and (d, e) ubiquitin microcrystals (a, d) without and (b, e) with 10 mM Cu-EDTA, where only the aliphatic region of the spectra are displayed for clarity. The spectra in (c, f) show the difference between the spectra without and with Cu-EDTA for (c) lysozyme and (f) ubiquitin. As discussed above, in (b, e), no major changes were observed by the addition of 10 mM Cu-EDTA. Although  $^1\text{H } T_1$  values were reduced by factors of (b) 8.3 and (e) 13.7, the line broadening is only subtle (10-20 %). However, we observed that a few resonances observed in Fig. 5(a, d) are substantially reduced in intensity in the spectra in (b, e) (indicated by arrows). The quenched signals may be assigned to residues exposed to the protein surface, at which  $^{13}\text{C}$  spins can be subject to much faster paramagnetic  $T_2$  relaxation due to Cu-EDTA in water phase. It is known that paramagnetic  $^{13}\text{C } T_2$  relaxation rates are proportional to  $1/R^6$ , where  $R$  is the distance between a  $^{13}\text{C}$  spin and a paramagnetic ion.[45;46] Hong *et al.* reported that the paramagnetic quenching can be utilized to measure distances of  $^{13}\text{C}$  sites in membrane bound peptides from the membrane surface with ranging Mn(II) concentration in water phase.[46] Thus, it is probable that signals for residues exposed to the protein surface are selectively quenched by the paramagnetic effects, while the majority of signals for other residues are unaffected. Further studies are needed to examine the possibilities of using the effects for structural analysis. The difference spectra in (c, f) also suggest that the effects of paramagnetic quenching are relatively minor; the integral intensities of (c) and (f) are only 2 and 11 % of those for (a) and (d), respectively. Considering that the amount of the proteins may differ by 5-10 % between (d) and (e) (or (a) and (b)), the overall signal quenching due to the Cu(II) addition is less than the significant level. We also found that the resolution in  $^{13}\text{C}$  CPMAS spectrum of lysozyme was not substantially degraded by the addition of 75 mM Cu-EDTA (data not shown). The  $^1\text{H } T_1$  value in this condition is about 27 ms, which is one tenth of the  $^1\text{H } T_1$  for the same protein without Cu-EDTA. Therefore, for the majority of the signals, further sensitivity enhancement is possible with more optimized pulse sequences for this purpose.

## Conclusion

In this study, we demonstrated that  $^1\text{H } T_1$  values of the two model proteins, lysozyme and ubiquitin, in microcrystals can be reduced to ~60 ms by Cu-EDTA doping without major degradation in the resolution of their  $^{13}\text{C}$  CPMAS spectra. We also demonstrated that significant sensitivity enhancements of 1D  $^{13}\text{C}$  CPMAS spectra were attained for these proteins by faster signal repetitions using the reduced  $^1\text{H } T_1$  values under fast MAS. Although the full potential of this approach for sensitivity enhancement is still restricted only in the fast MAS condition, our study presented a new opportunity to gain significant sensitivity enhancements using paramagnetic doping in biomolecular SSNMR. In this communication, we focused on testing this approach in 1D  $^{13}\text{C}$  CPMAS for unlabeled ubiquitin and lysozyme microcrystals. It is probable that the present approach can be adopted in CPMAS or static experiments of other insoluble proteins. The successful reduction of  $^1\text{H } T_1$  relaxation times in the present experiments will also open new possibilities of sensitivity enhancements in more advanced experiments such as multi-dimensional  $^{13}\text{C}$  SSNMR of uniformly  $^{13}\text{C}$ -labeled proteins [18-25] and various distance measurements[3;11;13;47-50] for selectively  $^{13}\text{C}$ -labeled protein samples in our future studies.

## Acknowledgement

We thank Dr. Siegfried Hafner at Varian Germany for helpful discussion on the  $\pi$ -pulse decoupling scheme under fast MAS. This work was supported in part by the Alzheimer's Association (NIRG 035123), the Dreyfus Foundation

Teacher-Scholar Award program, the NSF CAREER program (CHE 449952), the NIH/NIA RO1 grant (1R01 AG028490-01) for YI, and EU PF6 UPMAN project for AS.

## References

1. Opella SJ. NMR and membrane proteins. *Nat. Struct. Biol* 1997;4:845–848. [PubMed: 9377156]
2. Wildman KAH, Lee DK, Ramamoorthy A. Mechanism of lipid bilayer disruption by the human antimicrobial peptide, LL-37. *Biochemistry* 2003;42:6545–6558. [PubMed: 12767238]
3. Yang J, Weliky DP. Solid-state nuclear magnetic resonance evidence for parallel and antiparallel strand arrangements in the membrane-associated HIV-1 fusion peptide. *Biochemistry* 2003;42:11879–11890. [PubMed: 14529300]
4. Opella SJ, Marassi FM. Structure determination of membrane proteins by NMR spectroscopy. *Chem. Rev* 2004;104:3587–3606. [PubMed: 15303829]
5. Grant CV, Frydman V, Harwood JS, Frydman L. Co-59 solid-state NMR as a new probe for elucidating metal binding in polynucleotides. *J. Am. Chem. Soc* 2002;124:4458–4462. [PubMed: 11960475]
6. Griffin RG. Dipolar recoupling in MAS spectra of biological solids. *Nat. Struct. Biol* 1998;5:508–512. [PubMed: 9665180]
7. McDermott AE. Structural and dynamic studies of proteins by solid-state NMR spectroscopy: rapid movement forward. *Curr. Opin. Struct. Biol* 2004;14:554–561. [PubMed: 15465315]
8. Baldus M. Solid-state NMR spectroscopy: Molecular structure and organization at the atomic level. *Angew. Chem. Int. Edit* 2006;45:1186–1188.
9. Hong M. Resonance assignment of C-13/N-15 labeled solid proteins by two- and three-dimensional magic-angle-spinning NMR. *J. Biomol. NMR* 1999;15:1–14. [PubMed: 10549131]
10. Antzutkin ON, Balbach JJ, Leapman RD, Rizzo NW, Reed J, Tycko R. Multiple quantum solid-state NMR indicates a parallel, not antiparallel, organization of beta-sheets in Alzheimer's beta-amyloid fibrils. *Proc. Natl. Acad. Sci. U. S. A* 2000;97:13045–13050. [PubMed: 11069287]
11. Ishii Y. 13C-13C dipolar recoupling under very fast magic angle spinning in solid-state NMR: Applications to distance measurements, spectral assignments, and high-throughput secondary-structure elucidation. *J. Chem. Phys* 2001;114:8473–8483.
12. Petkova A, Ishii Y, Balbach JJ, Antzutkin ON, Leapman RD, Delaglio F, Tycko R. A structural model for Alzheimer's b-amyloid peptide fibrils based on experimental constraints from solid-state NMR spectroscopy. *Proc. Natl. Acad. Sci. U.S.A* 2002;99:16742–16747. [PubMed: 12481027]
13. Gullion T, Kishore R, Asakura T. Determining dihedral angles and local structure in silk peptide by C-13-H-2 REDOR. *J. Am. Chem. Soc* 2003;125:7510–7511. [PubMed: 12812479]
14. Chimon S, Ishii Y. Capturing intermediate structures of Alzheimer's b-amyloid, Ab(1-40), by solid-state NMR spectroscopy. *J. Am. Chem. Soc* 2005;127:13472–13473. [PubMed: 16190691]
15. Heise H, Hoyer W, Becker S, Andronesi OC, Riedel D, Baldus M. Molecular-level secondary structure, polymorphism, and dynamics of full-length alpha-synuclein fibrils studied by solid-state NMR. *Proc. Natl. Acad. Sci. U. S. A* 2005;102:15871–15876. [PubMed: 16247008]
16. Siemer AB, Ritter C, Ernst M, Riek R, Meier BH. High-resolution solid-state NMR spectroscopy of the prion protein HET-s in its amyloid conformation. *Angew. Chem. Int. Edit* 2005;44:2441–2444.
17. Martin RW, Zilm KW. Preparation of protein nanocrystals and their characterization by solid state NMR. *J. Magn. Reson* 2003;165:162–174. [PubMed: 14568526]
18. Castellani F, van Rossum B, Diehl A, Schubert M, Rehbein K, Oschkinat H. Structure of a protein determined by solid-state magic-angle- spinning NMR spectroscopy. *Nature* 2002;420:98–102. [PubMed: 12422222]
19. Bockmann A, Lange A, Galinier A, Luca S, Giraud N, Juy M, Heise H, Montserret R, Penin F, Baldus M. Solid state NMR sequential resonance assignments and conformational analysis of the 2 × 10.4 kDa dimeric form of the Bacillus subtilis protein Crh. *J. Biomol. NMR* 2003;27:323–339. [PubMed: 14512730]
20. Marulanda D, Tasayco ML, McDermott A, Cataldi M, Arriaran V, Polenova T. Magic angle spinning solid-state NMR spectroscopy for structural studies of protein interfaces. Resonance assignments of differentially enriched Escherichia coli thioredoxin reassembled by fragment complementation. *J. Am. Chem. Soc* 2004;126:16608–16620. [PubMed: 15600367]

21. Paulson EK, Morcombe CR, Gaponenko V, Dancheck B, Byrd RA, Zilm KW. High-sensitivity observation of dipolar exchange and NOEs between exchangeable protons in proteins by 3D solid-state NMR spectroscopy. *J. Am. Chem. Soc* 2003;125:14222–14223. [PubMed: 14624539]
22. Franks WT, Zhou DH, Wylie BJ, Money BG, Graesser DT, Frericks HL, Sahota G, Rienstra CM. Magic-angle spinning solid-state NMR spectroscopy of the beta 1 immunoglobulin binding domain of protein G (GB1): N-15 and C-13 chemical shift assignments and conformational analysis. *J. Am. Chem. Soc* 2005;127:12291–12305. [PubMed: 16131207]
23. Pauli J, Baldus M, van Rossum B, de Groot H, Oschkinat H. Backbone and side-chain C-13 and N-15 signal assignments of the alpha-spectrin SH3 domain by magic angle spinning solid-state NMR at 17.6 tesla. *Chembiochem* 2001;2:272–281. [PubMed: 11828455]
24. Giraud N, Bockmann A, Lesage A, Penin F, Blackledge M, Emsley L. Site-specific backbone dynamics from a crystalline protein by solid-state NMR spectroscopy. *J. Am. Chem. Soc* 2004;126:11422–11423. [PubMed: 15366872]
25. Lesage A, Emsley L, Penin F, Bockmann A. Investigation of dipolar-mediated water-protein interactions in microcrystalline Crh by solid-state NMR spectroscopy. *J. Am. Chem. Soc* 2006;128:8246–8255. [PubMed: 16787089]
26. Stringer JA, Bronnimann CE, Mullen CG, Zhou DHH, Stellfox SA, Li Y, Williams EH, Rienstra CM. Reduction of RF-induced sample heating with a scroll coil resonator structure for solid-state NMR probes. *J. Magn. Reson* 2005;173:40–48. [PubMed: 15705511]
27. Martin RW, Paulson EK, Zilm KW. Design of a triple resonance magic angle sample spinning probe for high field solid state nuclear magnetic resonance. *Review of Scientific Instruments* 2003;74:3045–3061.
28. Ernst M, Samoson A, Meier BH. Low-power decoupling in fast magic-angle spinning NMR. *Chem. Phys. Lett* 2001;348:293–302.
29. Ishii Y, Tycko R. Sensitivity enhancement in solid state <sup>15</sup>N NMR by indirect detection with high-speed magic angle spinning. *J. Magn. Reson* 2000;142:199–204. [PubMed: 10617453]
30. Long HW, Tycko R. Biopolymer conformational distributions from solid-state NMR: alpha-helix and 3(10)-helix contents of a helical peptide. *J. Am. Chem. Soc* 1998;120:7039–7048.
31. Iwahara J, Anderson DE, Murphy EC, Clore GM. EDTA-derivatized deoxythymidine as a tool for rapid determination of protein binding polarity to DNA by intermolecular paramagnetic relaxation enhancement. *J. Am. Chem. Soc* 2003;125:6634–6635. [PubMed: 12769564]
32. Samoson, A. Extended magic-angle spinning. In: Grant, DM.; Harris, RK., editors. *Encyclopedia of Nuclear Magnetic Resonance*. John Wiley & Sons, Ltd; New York: 2002. p. 59-64.
33. Samoson A, Tuherm T, Past J. Rotation sweep NMR. *Chem. Phys. Lett* 2002;365:292–299.
34. Samoson, A.; Tuherm, T.; Past, J.; Reinhold, A.; Anupold, T.; Heinmaa, N. New horizons for magic-angle spinning NMR. In: J., K., editor. *New Techniques in Solid-State Nmr*. Springer-Verlag; Berlin Heidelberg: 2005. p. 15-31.
35. Metz G, Wu X, Smith SO. Ramped-amplitude cross polarization in magic-angle-spinning NMR. *J. Magn. Reson. A* 1994;110:219–27.
36. Bennett AE, Rienstra CM, Auger M, Lakshmi KV, Griffin RG. Heteronuclear decoupling in rotating solids. *J. Chem. Phys* 1995;103:6951–8.
37. Ishii Y, Chimon S, Wickramasinghe NP. A new approach in 1D and 2D <sup>13</sup>C high resolution solid-state NMR spectroscopy of paramagnetic organometallic complexes by very fast magic-angle spinning. *J. Am. Chem. Soc* 2003;125:3438–3439. [PubMed: 12643699]
38. Wickramasinghe NP, Ishii Y. Sensitivity enhancement, assignment, and distance measurement in <sup>13</sup>C solid-state NMR spectroscopy for paramagnetic systems under fast magic angle spinning. *J. Magn. Reson* 2006;181:233–243. [PubMed: 16750405]
39. Ishii, Y.; Wickramasinghe, NP. 1H and <sup>13</sup>C high-resolution solid-state NMR of paramagnetic compounds under Very Fast Magic Angle Spinning. In: Webb, G., editor. *Modern Magnetic Resonances*; Springer, Berlin: In press
40. Hafner, S.; Palmer, A.; Cormos, M. Pulsed Heteronuclear Decoupling under Ultra-Fast Magic-Angle Spinning. *ENC* 2006; Asilomar, CA: 2006.
41. Liu SF, Schmidt-Rohr K. High-resolution solid-state C-13 NMR of fluoropolymers. *Macromolecules* 2001;34:8416–8418.

42. Morcombe CR, Gaponenko V, Byrd RA, Zilm KW. C-13 CPMAS spectroscopy of deuterated proteins: CP dynamics, line shapes, and T-1 relaxation. *J. Am. Chem. Soc* 2005;127:397–404. [PubMed: 15631490]
43. Igumenova TI, McDermott AE, Zilm KW, Martin RW, Paulson EK, Wand AJ. Assignments of carbon NMR resonances for microcrystalline ubiquitin. *J. Am. Chem. Soc* 2004;126:6720–6727. [PubMed: 15161300]
44. Abragam, A. Principles of nuclear magnetism. Oxford University Press; New York: 1961.
45. Solomon I. Relaxation processes in a system of two spins. *Phys. Rev* 1995;99:559–565.
46. Buffy JJ, Hong T, Yamaguchi S, Waring AJ, Lehrer RI, Hong M. Solid-state NMR investigation of the depth of insertion of protegrin-1 in lipid bilayers using paramagnetic Mn<sup>2+</sup> *Biophys. J* 2003;85:2363–2373. [PubMed: 14507700]
47. Gullion T, Schaefer J. Rotational-echo double resonance NMR. *J. Magn. Reson* 1989;81:196–200.
48. Long JR, Shaw WJ, Stayton PS, Drobny GP. Structure and dynamics of hydrated statherin on hydroxyapatite as determined by solid-state NMR. *Biochemistry* 2001;40:15451–15455. [PubMed: 11747419]
49. Antzutkin ON, Leapman RD, Balbach JJ, Tycko R. Supramolecular structural constraints on Alzheimer's beta-amyloid fibrils from electron microscopy and solid-state nuclear magnetic resonance. *Biochemistry* 2002;41:15436–15450. [PubMed: 12484785]
50. Jaroniec CP, Tounge BA, Herzfeld J, Griffin RG. Frequency selective heteronuclear dipolar recoupling in rotating solids: Accurate C-13-N-15 distance measurements in uniformly C-13,N-15-labeled peptides. *J. Am. Chem. Soc* 2001;123:3507–3519. [PubMed: 11472123]
51. Gullion T. The effect of amplitude imbalance on compensated Carr-Purcell Sequence. *J. Magn. Reson. A* 1993;101:320–323.



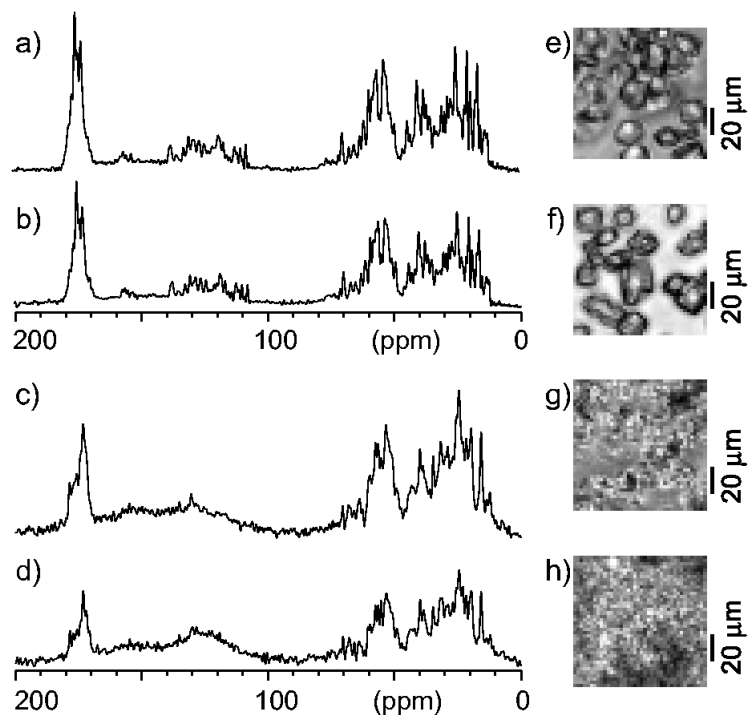


**Figure 1.** (a-d)  $^{13}\text{C}$  CPMAS spectra of protein crystals for (a, b) lysozyme and (c, d) ubiquitin prepared in  $\text{D}_2\text{O}$  obtained (a, c) with and (b, d) without 10mM Cu-EDTA at  $^{13}\text{C}$  NMR frequency of 100.6 MHz. The recycle delays were set to (a) 0.5 s, (b) 1.1 s, (c) 1.0 s, and (d) 2.5 s. The spectra were acquired at a spinning speed of 10 kHz under  $^1\text{H}$  TPPM decoupling of (a, b) 71 kHz and (c, d) 90 kHz. Signals were accumulated during acquisition periods of 10 ms with (a) 28160, (b) 12800, (c) 14336, and (d) 5736 scans in a common total experimental time of 4 hours. During the CP period of 1.0 ms,  $^{13}\text{C}$  RF field was swept (a, b) from 56 kHz to 76 kHz and (c, d) from 52 kHz to 72 kHz, while  $^1\text{H}$  RF field was kept at (a, b) 76 kHz and (c, d) 72 kHz. All the spectra were processed with Gaussian line broadening of 25 Hz. At the right of the spectra in (a-d), microscope images of the corresponding protein micro/nano-crystals used for the NMR experiments are displayed in (e-h). The images were obtained at 32 $\times$  magnification.

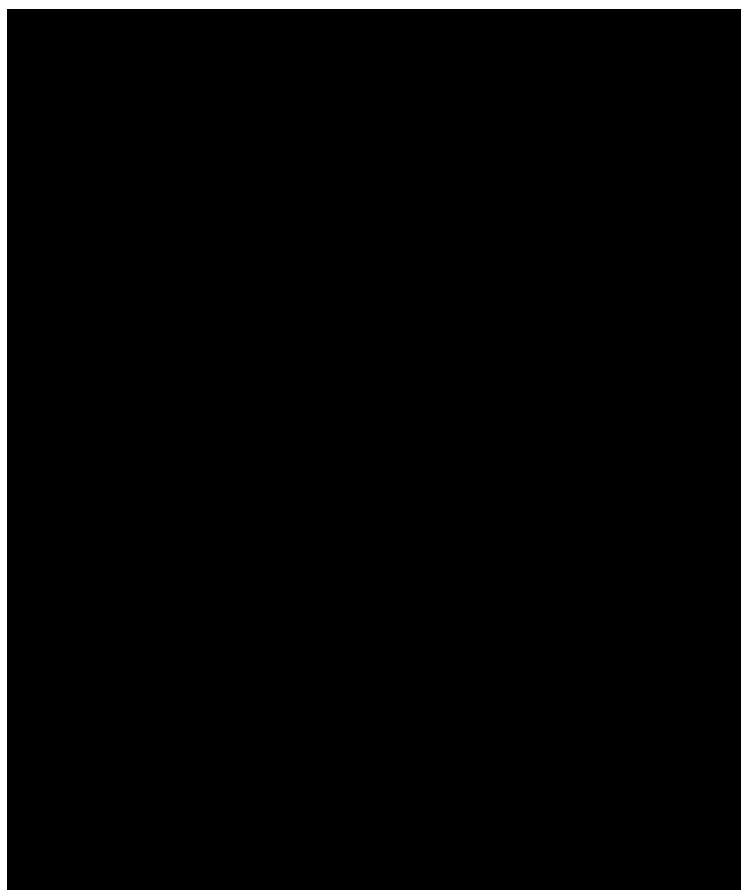


**Figure 2.** (a-d)  $^{13}\text{C}$  CPMAS spectra of protein micro crystals for (a, b) lysozyme and (c, d) ubiquitin prepared in  $\text{D}_2\text{O}$  obtained (a, c) with and (b, d) without 10 mM Cu-EDTA at  $^{13}\text{C}$  NMR frequency of 100.6 MHz. The recycle delays were (a) 0.18 s, (b) 1.50 s, (c) 0.18 s, and (d) 2.50 s. The spectra were acquired at a spinning speed of 40 kHz with  $\pi$ -pulse-train decoupling. In the decoupling scheme, a  $\pi$ -pulse with the width of 2.5  $\mu\text{s}$  was rotor-synchronously applied at the end of every rotor cycle (25  $\mu\text{s}$ ) with the XY-8 phase cycle.[51] Signals were accumulated during acquisition periods of 20 ms with (a) 36,000, (b) 4,800, (c) 72,000, and (d) 5,680 scans in a common total experimental time of (a, b) 2 hours or (c, d) 4 hours. During the CP period of 1.0 ms, the  $^{13}\text{C}$  RF field was swept from 53 kHz to 71 kHz, while the  $^1\text{H}$  RF field was kept at 102 kHz. All the spectra were processed with Gaussian line broadening of 15 Hz.

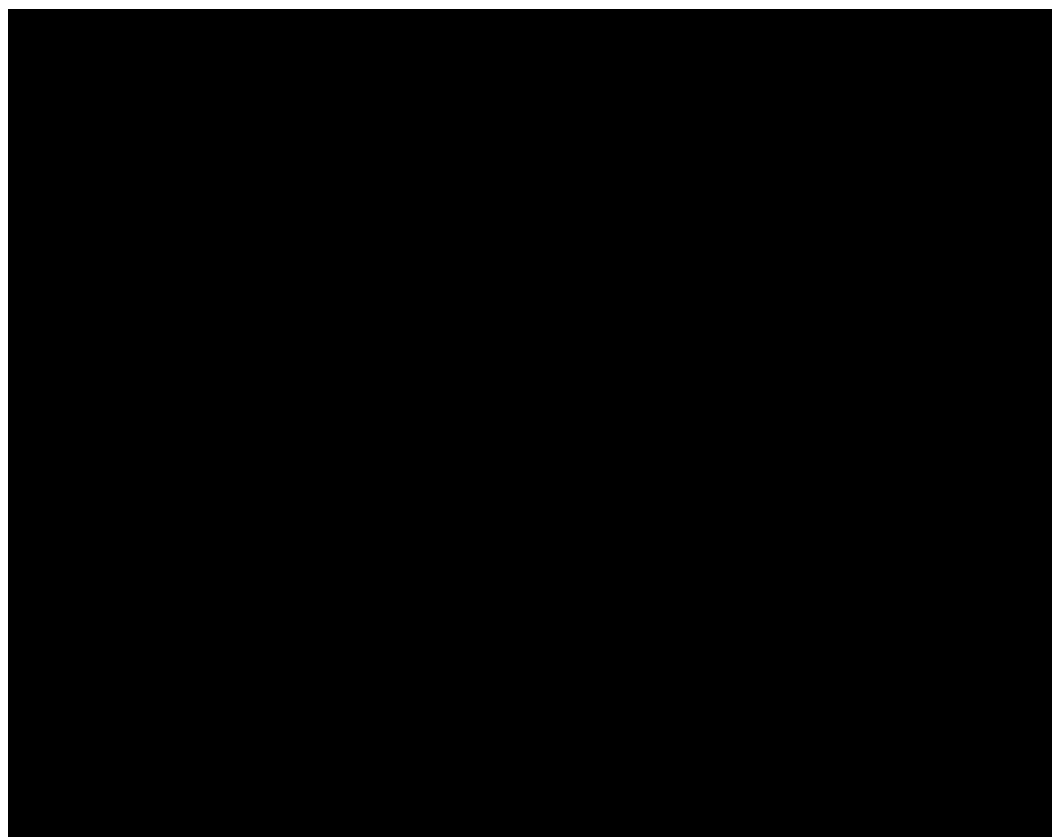


**Figure 3.**  $^1\text{H}$  inversion recovery delay ( $\tau_{\text{IR}}$ ) dependence of  $^{13}\text{C}$  CPMAS spectra of ubiquitin microcrystals prepared in  $\text{D}_2\text{O}$  (a) without and (b) with 10 mM Cu-EDTA obtained at 10 kHz MAS. The values of  $\tau_{\text{IR}}$  used in the experiments are indicated in the figure.

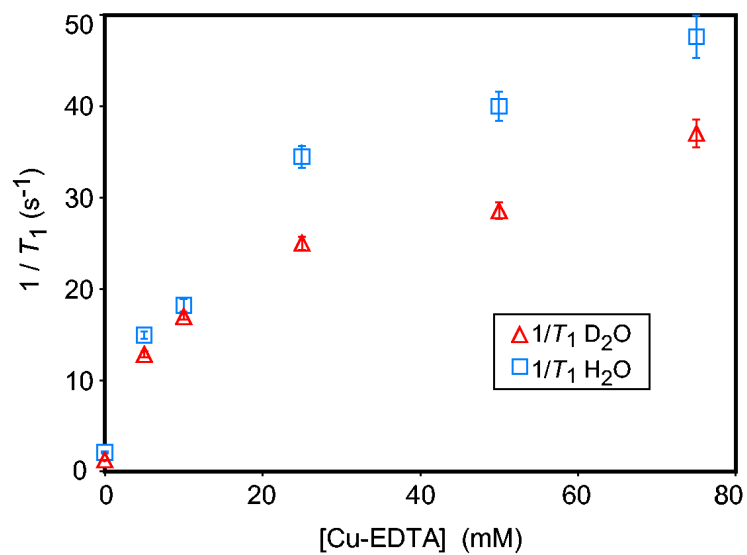


**Figure 4.** Cu-EDTA concentration dependence of the <sup>1</sup>H relaxation rate ( $1/T_1$ ) for lysozyme microcrystals prepared in D<sub>2</sub>O (triangle) and H<sub>2</sub>O (square). The <sup>1</sup>H  $T_1$  values were measured by the inversion recovery experiment shown in Fig. 3. The error bars indicate standard errors in the measurements of  $1/T_1$ .

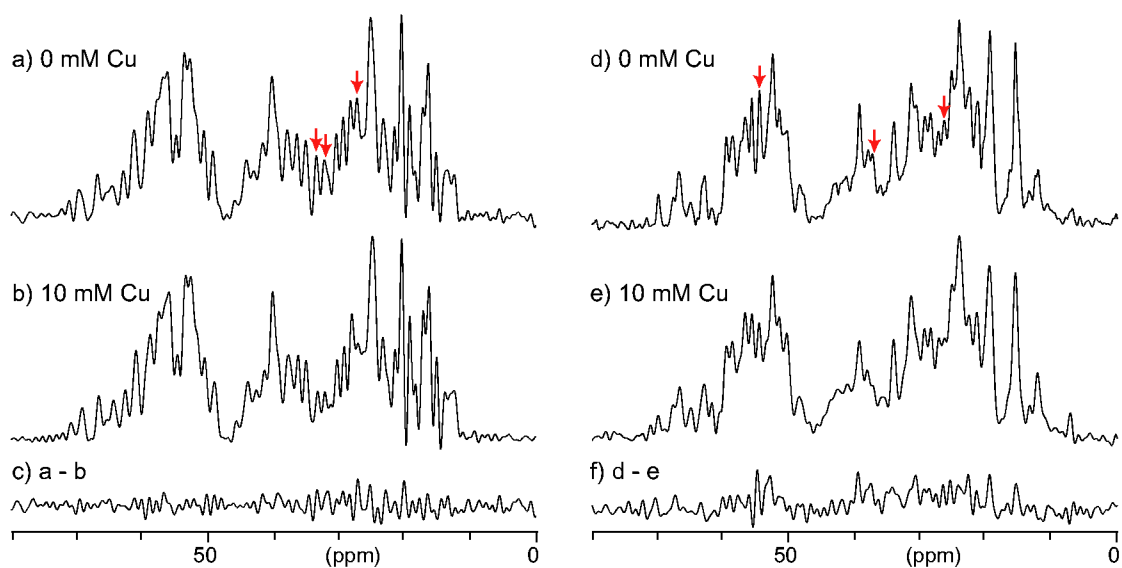


**Figure 5.**

$^{13}\text{C}$  CPMAS spectra of (a, b) lysozyme and (d, e) ubiquitin protein crystals with Cu-EDTA concentrations of (a, d) 0 mM, (b, e) 10 mM. The spectra in (c, f) are the difference between the spectra obtained with and without Cu-EDTA for the same sample. The spectra were obtained at  $^{13}\text{C}$  NMR frequency of 100.6 MHz at a spinning speed of 40 kHz with  $^1\text{H}$   $\pi$  pulse-train decoupling during the acquisition periods of 10 ms. The shorter acquisition periods were adopted to minimize the noise level for comparison. The recycle delays were (a) 1.50 s, (b) 0.18 s, (d) 2.50 s, and (e) 0.18 s. All the spectra were processed with Gaussian line broadening of 25 Hz.

$^1\text{H } T_1$  values of ubiquitin and lysozyme in the presence and absence of Cu-EDTA with their approximate crystal sizes measured from microscopic images.

**Table 1**

Protein	Crystal size ( $\mu\text{m}$ )	$^1\text{H } T_1^{\text{D}_2\text{O}}$ (ms) <sup>a</sup>	$^1\text{H } T_1^{\text{H}_2\text{O}}$ (ms) <sup>b</sup>	With Cu-EDTA in $\text{D}_2\text{O}$	
				[Cu-EDTA] (mM)	$^1\text{H } T_1$ (ms) <sup>c</sup>
Ubiquitin	1-5	820 $\pm$ 10	307 $\pm$ 19	10	73 $\pm$ 1
Lysozyme	5-20	350 $\pm$ 4	280 $\pm$ 5	10	59 $\pm$ 1

<sup>a</sup> $^1\text{H } T_1$  for the sample prepared in  $\text{D}_2\text{O}$  used for Fig. 1 (b, d).  $^1\text{H } T_1$  values were 500 and 820 ms for Fig. 2(b), (d), respectively.

<sup>b</sup> $^1\text{H } T_1$  for the sample prepared in  $\text{H}_2\text{O}$ .

<sup>c</sup> $^1\text{H } T_1$  for the sample used for Fig. 1 (a, c).  $^1\text{H } T_1$  values were 60 ms for both Fig. 2(a) and (c).